

UC Riverside

UCR Honors Capstones 2016-2017

Title

Understanding the Role of Perineuronal Nets in Developing Hippocampal Circuits in a Mouse Model of Fragile X Syndrome

Permalink

<https://escholarship.org/uc/item/7rb4x65r>

Author

Espinoza, Katherine

Publication Date

2017-12-08

UNDERSTANDING THE ROLE OF PERINEURONAL NETS IN DEVELOPING
HIPPOCAMPAL CIRCUITS IN A MOUSE MODEL OF FRAGILE X SYNDROME

By

Katherine Espinoza

A capstone project submitted for
Graduation with University Honors

May 11, 2017

University Honors
University of California, Riverside

APPROVED

Dr. Iryna Ethell
Department of Biomedical Sciences

Dr. Richard Cardullo, Howard H Hays Jr. Chair and Faculty Director, University Honors
Interim Vice Provost, Undergraduate Education

ABSTRACT

Fragile X Syndrome (FXS) is a leading cause of intellectual disability and autism. It is caused by an expansion of CGG repeats that leads to hypermethylation and silencing of Fragile X Mental Retardation (*Fmr1*) gene. Silencing of the *Fmr1* gene results in the loss of Fragile X Mental retardation protein (FMRP), which can cause abnormal synaptic transmission. These deficits contribute to various FXS symptoms, including cognitive and learning impairments. However, the origins of these deficits remain unknown. *Fmr1* KO mice were used in this study to understand the mechanisms of learning impairments in FXS. The FXS *Fmr1* KO mouse model exhibits an excitatory-inhibitory (E/I) imbalance, which suggest abnormal synaptic functions in areas such as the hippocampus, area of the brain responsible for learning. Previous studies in *Fmr1* KO mice have demonstrated an increase in levels of matrix metalloproteinase-9 (MMP-9), an extracellular enzyme that cleaves extracellular matrix (ECM), including perineuronal nets (PNNs) and can affect synaptic transmission. PNNs act as scaffolds around inhibitory neurons, such as parvalbumin (PV) positive cells, to regulate their activity. Based on this evidence, the goal of this study is to determine if there is abnormal development of PV positive cells and PNNs in the hippocampus of *Fmr1* KO mice. We hypothesized that if MMP-9 levels are elevated with FXS, genetic reduction of MMP-9 may reverse the deficits. The results of this pilot study indicate reduced density of PV cells in the CA1 subfield of the hippocampus in the *Fmr1* KO mice compared to the WT mice. The results of this study may provide new insight into E/I imbalance in autism spectrum disorders and into the mechanisms of abnormal hippocampal development that may lead to learning deficits in FXS.

ACKNOWLEDGMENTS

This Honors Capstone Project would have not been possible without the help of the following people:

- Dr. Iryna Ethell
- Dr. Sonia Afroz
- Ethell Lab: Teresa, Sarah, Amanda, Arnold, Anna, Jordan
- University of California, Riverside
 - Academic Resource Center
 - Department of Biomedical Sciences
 - University Honors Program
 - Neuroscience Undergraduate Program

Thank you.

TABLE OF CONTENTS

Title page	i
Abstract.....	ii
Acknowledgments	iii
Table of Contents.....	iv
List of Figures	v
Introduction.....	1
- Fragile X Syndrome.....	1
- Hippocampus	3
- Inhibitory Interneurons	7
- Perineuronal nets.....	8
- Matrix metalloproteinase	10
Purpose.....	11
Methods and Materials	11
Results.....	14
Discussion.....	20
Future Directions	22
References.....	23

LIST OF FIGURES

Figure 1.	3
Figure 2.	6
Figure 3.	9
Figure 4.	15
Figure 5.	17
Figure 6A-B.	18
Figure 6C-D.	19

INTRODUCTION

Fragile X Syndrome

Fragile X syndrome (FXS) is a form of intellectual disability and it is the most common cause of autism and mental retardation (Spencer et al., 2011). This is a disorder that results from an expansion of a trinucleotide repeat (CGG) in a region on the X chromosome that contains the Fragile X Mental Retardation (*Fmr1*) gene (Kazdoba et al., 2014). The expansion ranges from normal, 40-50 trinucleotide repeats, to a mutation with more than 200 repeats in the 5' untranslated region of the *Fmr1* gene (Garber et al., 2008). Full mutation of CGG repeats can cause hypermethylation and transcriptional silencing of the *Fmr1* promoter, resulting in the absence of the Fragile X Mental retardation protein (FMRP) (Wang et al., 2010). FMRP binds to RNA that functions in translating polyribosomes and plays a role in regulating protein synthesis (Qin et al., 2005). The RNA-binding ability of FMRP suggests that it can affect protein levels by regulating translation of specific mRNA (Dolen et al., 2010), affecting synaptic functions that can explain cognitive deficits observed in human subjects with FXS.

FXS is found in about 1 in 4000 men compared to 1 in 6000 women (Smit et al., 2008). Common characteristics of FXS include hyperactivity, hypersensitivity to sensory stimuli, and attention, and learning deficits (Smit et al., 2008; Spencer et al., 2011). To better understand the deficits of FXS, the first mouse model lacking FMRP (*Fmr1* KO) was created in 1994 by Dutch-Belgian Fragile X Consortium. The *Fmr1* KO mice lack FMRP similar to human subjects with FXS. Studies in the *Fmr1* KO mouse have shown cognitive deficits related to working memory when compared to the wild-type mice

which exhibit normal levels of FMRP (Kazdoba et al., 2014). Associative learning tasks in mammals, which include eyeblink conditioning, have been used to understand the cognitive deficits associated with autism spectrum disorders. Eyeblink conditioning is a form of classical conditioning that is a process by which behaviors are acquired with repeated pairing of unconditioned stimuli (Encyclopedia of Adolescence, 2011). This form of conditioning is associated with the motor nuclei, cerebellum and hippocampus (Poulos et al., 2008). An experiment conducted by Smit and colleagues measured responses to paired tone and air puff stimuli in males with FXS. They concluded that the subjects had a form of learning impairment, specifically, males with FXS showed less conditioned response during the acquisition phase. The study showed that a loss of FMRP influences the associative learning in males with FXS (Smit et al., 2008).

Learning deficits in FXS may associate with abnormal development of the hippocampal circuits, as a study testing two hippocampus-dependent learning paradigms: contextual fear conditioning and passive avoidance examination, indicated a difference in *Fmr1* KO versus wild-type mice (Q. Ding et al., 2014). During the contextual fear conditioning, the *Fmr1* KO mice exhibited less freezing compared the WT (Q. Ding et al., 2014). In the passive avoidance-testing period, crossover latency was measured as the time the mouse remained in the lit chamber once the trap door was opened. The *Fmr1* KO demonstrated a shorter crossover latency compared to the wild-type mice, indicating a possible effect on working memory after *Fmr1* KO (Q. Ding et al., 2014). Other studies showed that working memory is also affected in *Fmr1* KO mice during water maize training (Baker et al., 2010). These studies suggest a deficit in hippocampal-dependent learning tasks. Other studies observed no difference in three fear response conditions in mice with *Fmr1* KO

but did observe deficits in cross maze tasks (Dobkin et al., 2000). As a result, understanding the function of the hippocampus at the cellular level can serve to understand the changes that may occur in the *Fmr1* KO mouse model.

Hippocampus

Many of the behavioral deficits observed in the *Fmr1* KO mice are specific to the functions of the hippocampus. Contextual cues are processed in the hippocampus in an association with behavioral experiences and allow for discrimination between harmful or rewarding and neutral environments (Basu et al., 2016). It also plays a role in processes including memory/binding of complex associations (Till et al., 2015). Information from the entorhinal cortex, such as spatial information, is processed in the hippocampus through a synaptic loop (Neves et al., 2012). The hippocampus proper contains pyramidal cells and is divided into four areas: CA1, CA2, CA3 and CA4 (Johnston et al., 2004, Figure 1). The separate region of the hippocampus, dentate gyrus (DG), is made up of granule cells and receives input from the entorhinal cortex (Johnston et al., 2004). CA1 area is anatomically subdivided into four layers: stratum oriens, stratum pyramidale, stratum radiatum and stratum lacunosum moleculare (Figure 1). Layer II of the entorhinal cortex sends information to the granule cells of the dentate gyrus, and these axons project to the apical dendrites of CA3 and CA2 pyramidal cells which project their Schaffer collaterals to stratum radiatum layer of CA1 pyramidal cells (Neves et al., 2012; Figure 2), which then innervates another area of the hippocampus known as subiculum.

In this loop, the CA2 is a small region interposed between the CA3 and CA1 regions and is thought to receive excitatory inputs from layer III of the entorhinal cortex (Hitti et al., 2014). The CA2 region was thought to only play a role in social memory but recent

studies suggest that it may play a role in modulatory systems require for optimal sensory and mnemonic processing in the hippocampus (Caruana et al., 2017). The CA1 region is the main site that integrates excitatory input from the entorhinal cortex (stratum lacunosum moleculare layer) and from CA3 neurons (stratum radiatum layer) (Basu et al., 2016). This region plays a role in synaptic plasticity by enabling bursts of action potentials in response to a repetitive stimulation. Synaptic plasticity is a process in which associative networks of connections can be formed and can respond to changes in nervous system environment (Reinhard et al., 2014). These associations are formed by synapses of excitatory cells and are refined by inhibitory interneurons.

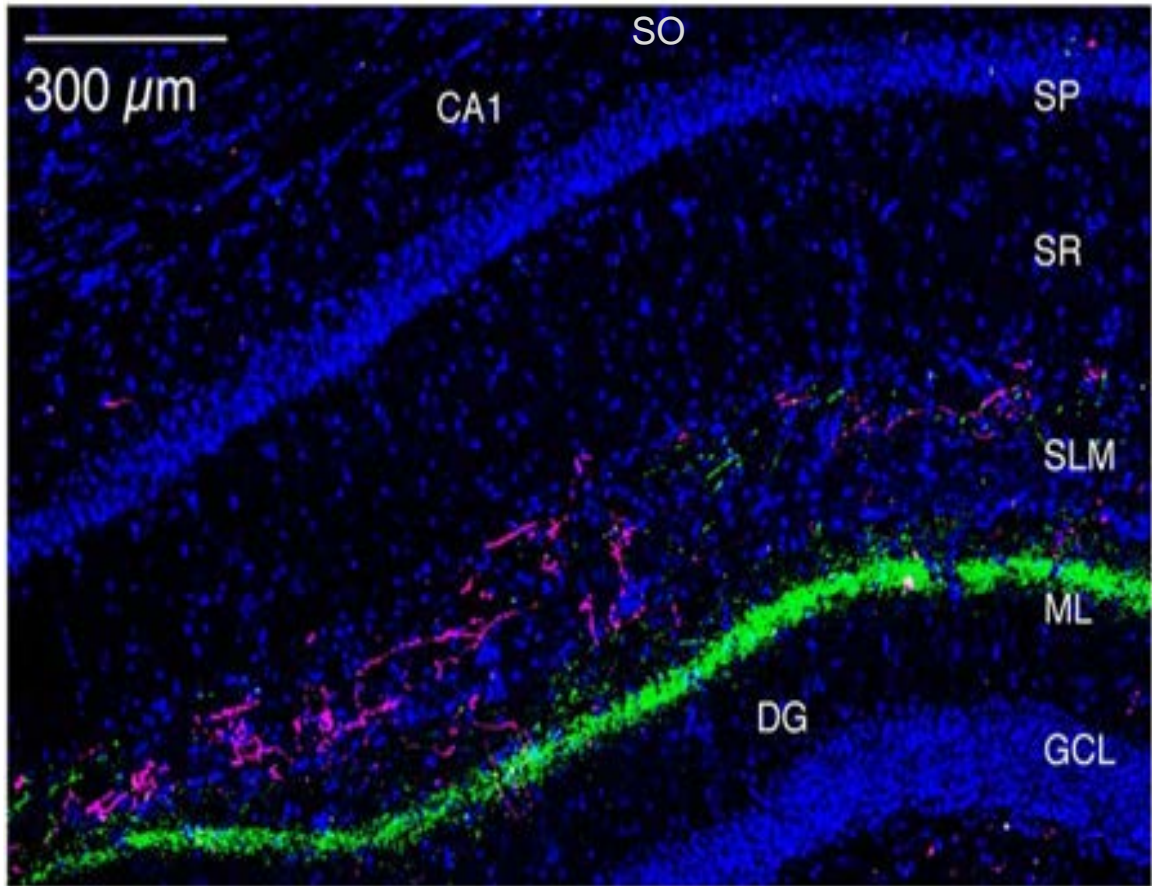


Figure 1. This is a hippocampal section indicating the strata of the CA1 in the hippocampus. SO is the stratum oriens which is the outermost layer. This layer contains basal dendrites from the pyramidal cells in the SP: stratum pyramidale is the pyramidal neuron cell body layer. SR: stratum radiatum is the layer that receives input from the CA3 region by projections called Schaffer collaterals. SLM: stratum lacunosum moleculare which receives inputs from the entorhinal cortex. The dentate gyrus (DG) is made up of the ML: molecular layer and GCL: granule cell layer which also receive input from the entorhinal cortex. (Source: Jayeeta Basu et al. Science 2016;351:aaa5694)

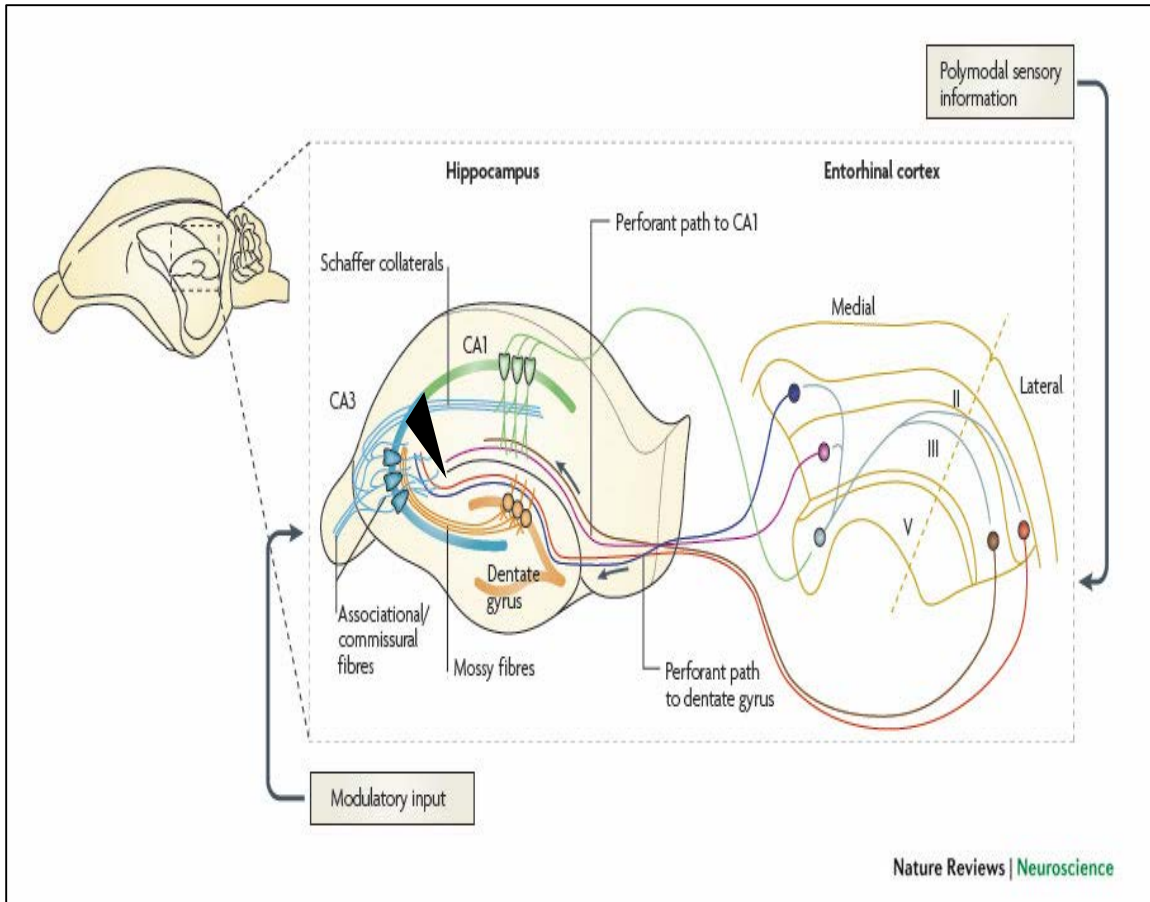


Figure 2. This figure describes the circuit involved in information processing in the different region of the hippocampus. Input from the entorhinal cortex projects on the perforant path to the CA1 region and to the granule cells in the dentate gyrus. The granule cells project their mossy fibers to the proximal apical dendrites of the CA3 region. The CA3 Schaffer collaterals project to the pyramidal cells of the CA1 region. The projections are to the ipsilateral CA1 pyramidal neurons and the contralateral CA1 neurons through the associational fibers. The CA2 region is indicated by the black triangle interposed between the CA3 and CA1 region. This region possesses pyramidal neurons that project onto the CA1 region. (Source: Nature Reviews Neuroscience 9, 65-75, January 2008).

Inhibitory interneurons

In the hippocampus, the main inhibitory neurotransmitter is γ -aminobutyric acid (GABA) and glutamate is the main excitatory neurotransmitter (Johnston and Amaral, 2004). A balance between excitatory and inhibitory inputs plays an important role in synaptic functions and plasticity. Synaptic plasticity is a mechanism that adjusts the synaptic strength of neural inputs (Hensch 2005). It is thought that the fundamental role of inhibitory interneurons is to stabilize the cortical circuits during critical period (Galaretta et al., 2001). The critical period is a developmental window in which essential cortical circuits are selected from the many synapses that form during early development to permanently alter performance (Hensch 2005). The hippocampus has different inhibitory interneurons that release GABA as their neurotransmitter. One type of interneurons localized in the hippocampus is parvalbumin (PV) expressing interneurons. The parvalbumin expressing GABAergic interneurons express calcium-binding protein called parvalbumin and are mostly perisomatic basket cells (Murray et al., 2015). Cell bodies of PV expressing interneurons are mostly found in the SP layer of the hippocampus and their dendrites project into the SLM layer. PV interneurons produce fast spiking inhibitory postsynaptic potentials due to their expression of μ -opioid receptors (Pawelzik et al., 2002). These opioid receptors are coupled to inhibitory G-proteins and potassium channels to produce inhibition in the hippocampus and to reduce excitation of CA1 neurons in a temporal and spatial manner (Hasani et al., 2011).

The PV positive cells are thought to play a role in excitatory-inhibitory (E/I) balance by offering a system sensitive to the timing of critical period plasticity (Fagiolini et al., 2004). Deficits in some models of autism are thought to be caused by an increased ratio

of excitation/inhibition in sensory, social, and mnemonic systems (Rubenstein et al., 2003). This imbalance of excitation and inhibition can be due to increased glutamatergic signaling or reduced GABAergic signaling (Rubenstein et al., 2003). One study using mouse models of autism spectrum disorders has shown a reduction of PV cells in the neocortex and the hippocampus in their autism model (Gogolla et al., 2009).

Perineuronal nets

PV positive cells are enwrapped in extracellular matrix (ECM) enriched in chondroitin sulfate proteoglycans (CSPGs) forming perineuronal nets (PNNs), which are thought to play a role in learning (Gogolla et al., 2009). The PNNs have a backbone composed of hyaluronic acid (HA) that is covalently bound to the CSPGs (Hylín et al., 2013; Figure 3). The function of PNNs is unknown but it is speculated to buffer the cationic environment surrounding the cells (Gogolla et al., 2009; Hartig et al., 1999). Studies of synaptic plasticity in visual cortex showed that a removal of CSPG side chains with chondroitinase-ABC (ChABC) reduced inhibitory properties of the central nervous system in adult mice enhancing synaptic plasticity (Pizzorusso et al., 2002). Although this is not specific to the hippocampus, this demonstrates that PNNs play a role in limiting synaptic plasticity and stabilization of synaptic connections. PNN colocalization with GABAergic PV positive cells has also been proposed to be involved in the closure of the critical plasticity period marking the maturation of cortical circuits (Pizzorusso et al., 2002). Thus, the extracellular matrix has been a focus in many studies because it seems to be a major regulator of synaptic plasticity in the cerebral cortex (Hensch 2005). PNN disruption in the hippocampus by ChABC and hyaluronidase has also been studied to understand the effects in long-term fear memory. Hippocampal plasticity is important

for contextual fear memory formation in fear conditioning tasks and removal of CSPG side chains cause a significant impairment in long-term contextual memory (Hylin et al., 2013). The CA1 area showed less PNN compared to other regions in the hippocampus but it was the area that contributes to memory impairments observed in mice treated with ChABC (Hylin et al., 2013). Studies have shown the CA2 area is highly enriched with PNNs indicated by intense labelling of Wisteria Floribunda Lectin, which is a plant protein that binds to CSPG side chains (Bruckner et al., 2003). These studies show that PNNs play a role in cognitive functions and understanding its function can lead to help identify the cause of the learning deficits associated with FXS.

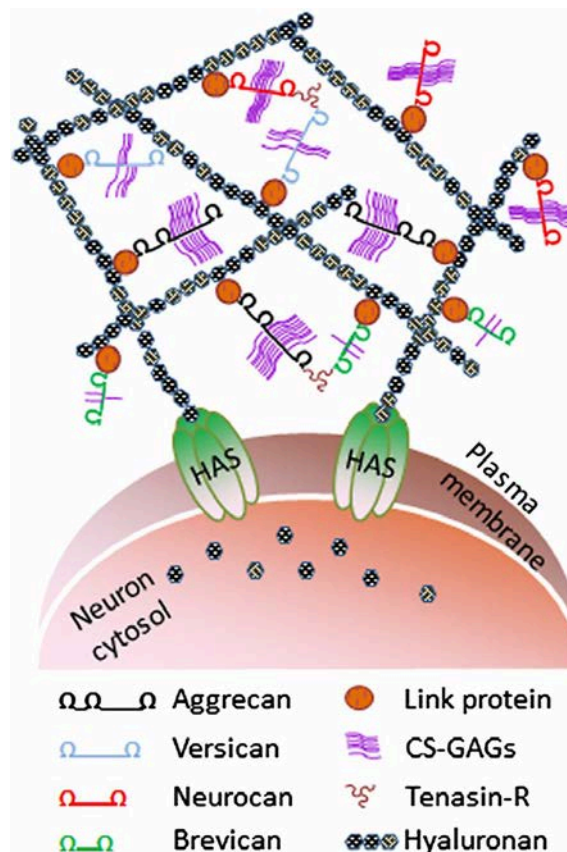


Figure 3. This figure diagrams the composition of perineuronal nets. It indicates that the backbone is made up of hyaluronic acid. It acts as the link to plasma membrane of the neuron. The CSPGS can covalently bind to the hyaluronic acid. (Source: Tsien Y. Roger, PNAS. 2013 Jul 5)

Matrix metalloproteinase-9

Unlike ChABC, which removes CSPG glycosaminoglycan side chains, matrix metalloproteinase 9 (MMP-9) cleaves the protein of the extracellular matrix such as PNNs and several surface receptors allowing synaptic organization (Reinhard et al., 2015). MMP-9 plays a role in the development of sensory circuits during early developmental periods and regulates circuit organization by controlling synaptogenesis (Ethell et al., 2007; Reinhard et al., 2015). Enhanced MMP9 activity has been associated with several neurodegenerative diseases and can also influence the functions of synaptic networks in neurodevelopmental disorders such as FXS by modifying surrounding extracellular matrix. MMP-9 levels are upregulated in the auditory cortex of adult *Fmr1* KO mice (Wen, et al. *In Preparation*) and this can be the cause of hypersensitivity to auditory stimuli (Lovelace et al., 2016). MMP-9 levels are also upregulated in hippocampus of adult KO mice (Sidhu et al., 2014). Post-mortem brain samples from patients with FXS also exhibit higher levels of MMP-9 compared to control subjects (Sidhu et al., 2014). In studies focusing on FXS-associated defects such as poor socialization, dendritic spine maturation, and enhanced long-term depression, mice lacking both FMRP and MMP9 exhibited normal behavior and morphologies comparable to the WT mice (Sidhu et al., 2014). These studies indicate that down-regulating MMP-9 levels may be also key in reversing learning deficits in *Fmr1* KO mice.

PURPOSE

Based on the knowledge known about FXS and its deficits, present studies have been performed to understand the underlying mechanisms of these deficits. Our goal was to

understand the cellular level changes in the hippocampus in *Fmr1* KO mice compared to WT mice, which may underlie learning and memory deficits. In this study, we characterized density of PV positive cells and PNN expression in the hippocampus of WT, *Fmr1* KO and MMP9/*Fmr1* DKO mice (Harris et al, 2005). Previous research indicates that there is less PV density in the hippocampus in mice modeling autism spectrum disorders (Gogolla et al., 2009). Other studies indicate that PNN levels are also reduced in the hippocampus following the ECM cleavage by ChABC (Hylin et al., 2013). These findings relate to mouse models of FXS because *Fmr1* KO mice are found to have increased levels of MMP-9 in the hippocampus and MMP-9 can cleave PNNs (Sidhu et al., 2015; Ethell et al., 2007). Therefore, I hypothesized that *Fmr1* KO mice would exhibit lower PV and PNN density in the hippocampus compared to the WT mice. Furthermore, genetic reduction of MMP-9 levels are tested to determine if this reduction is sufficient to restore PV cell density and PNN expression to WT levels.

MATERIALS AND METHODOLOGY

Mice

FVB.129P2-*Fmr1*^{tm1Cgr}/J (*Fmr1* KO) and FVB.129P2-Pde6b⁺Tyr^{c-ch}/AntJ controls (WT) mice from Jackson laboratories were housed in a vivarium on a 12-hour light/dark cycle. Food was provided *ad libitum*. The FVB.Cg-*Mmp-9*^{tm1Tvu}/J mice were backcrossed with *Fmr1* KO mice to generate *Mmp9*^{-/-}*Fmr1* KO and *Mmp9*^{+/-}*Fmr1* KO mice. Genomic DNA was isolated from mouse tails of litter from each cross and were purified. PCR analysis used to confirm the genotypes. The Institutional Animal Care and Use

Committee at the University of California, Riverside approved all procedures performed on mice.

Immunohistochemistry

At age P21, male WT, *Fmr1* KO, *Mmp9*^{+/-}*Fmr1* KO and *Mmp9*^{-/-}*Fmr1* KO mice were euthanized with isoflurane and perfused with 4% paraformaldehyde (PFA) and cold 0.1 M phosphate-buffered saline (PBS). Brains were removed and post-fixed in 4% PFA for 2-4 hours. The brains were sectioned to 100 µm slices using a vibratome (EMS 5000) at a speed of 3.5 and amplitude of 5.0-5.5. Hippocampus was identified based on location of the dentate gyrus and entorhinal cortex using *The Mouse Brain* by Paxinos and Franklin.

For each brain, an average of 5-6 slices containing the hippocampus were obtained.

Sections were labeled using the following immunohistochemistry protocol. Brain slices were post-fixed for 2 hours in 4% PFA in 0.1M PBS and then washed 3x in 0.1M PBS. Slices were quenched with 50 mM ammonium chloride for 15 minutes and washed with PBS. Then, brain tissues were permeabilized with 0.1% Triton X-100 in PBS and nonspecific binding was blocked with a 1% Bovine Serum Albumin (BSA; Fisher Scientific, catalog# 9048-46-8) and 5% Normal Goat Serum (NGS; Sigma, catalog# G9023-10mL) in 0.1M PBS solution. Next, primary antibodies and *Wisteria floribunda agglutinin* (WFA) in 0.1 M PBS containing 1% NGS, 0.5% BSA, and 0.1% Tween-20 solution were added to brain sections for 24 hours. WFA (4µg/ml; Vector Laboratories, cat# FL-1351, RRID:AB_2336875) binds to the chondroitin sulfate proteoglycan(CPSG) side chains and is an antibody for NH₂ terminals on CPSGs (Pizzorusso, 2002). Primary antibodies used include mouse anti-parvalbumin (1:1000; Sigma, catalog# P3088, RRID:AB_477329) to label PV interneurons. After incubating in the primary antibodies

and WFA solution slices were washed in 0.5% Tween-20 in 0.1 M PBS. Then, slices were incubated with secondary antibodies in 0.1M PBS for 1 hour. Secondary antibodies were donkey-anti rabbit Alexa 594 (4 μ g/ml; Thermo Fisher Scientific, catalog# A-21207, RRID:AB_141637), donkey anti-rabbit Alexa 647 (4 μ g/ml; Thermo Fisher Scientific, catalog# A-31573, RRID:AB_2536183) and donkey anti-mouse Alexa 594 (4 μ g/ml; Thermo Fisher Scientific, catalog# A-21203, RRID:AB_2535789). Next, slices were washed with 0.5% Tween-20 in 0.1M PBS and mounted with Vectashield containing DAPI (Vector Labs, catalog# H-1200) and sealed with Cytoseal (ThermoScientific, catalog# 8310-16).

Confocal microscopy image analysis

Slices were imaged by confocal microscopy using Leica SP5. Next, images were captured at 20 high-resolution (1550 x 1550-pixel format) using a 10x objective (1.2 numerical aperture), at 1.01 μ m step intervals. Each z-stack (20 μ m) was merged into a single image (LSM Image Browser, Image J), converted to an 8-bit TIFF file, and analyzed using Image J. PNN positive cells and PV positive cells were counted for the different regions of the hippocampus including CA1 proximal, CA1 distal, CA2, CA3, dentate gyrus. The freehand selection tool and measure function was used to specify the regions of the hippocampus and the point tool was used to label PNNs and PV cells. Each selection was added to the ROI manager. Particle Analysis Cell Counter plugin in Image J was used to count colocalization. One-way ANOVA and two-tailed t-test was used to determine genotype differences. Tukey's test was used for *post-hoc* analysis using Graph Pad Prism 6.

RESULTS

Immunohistochemistry Data

Studies have suggested that the levels of MMP-9 are elevated in the *Fmr1* KO mouse model (Sidhu et al., 2014). MMP-9 has been found to cleave the extracellular matrices such as PNNs (Ethell et al., 2007). My focus was to understand how the levels of PNN in hippocampus of WT and *Fmr1* KO differed. We captured images using confocal laser microscopy to observe the number of PNN in the different regions of the hippocampus (Figure 4). A difference was observed in the levels of PV cells between the wildtype and *Fmr1* KO. Images in Figures 4a and 4b support the hypothesis that PNN levels should be less in the *Fmr1* KO due to the upregulation of MMP-9. Interestingly, the PNN levels in the DKO were the same as the levels observed in the *Fmr1* KO (Figure 4b-4c). The DKO has a deletion of MMP-9 and is also an *Fmr1* KO. We hypothesized that due to the deletion of MMP-9, there should be an increase or maintain the same PNN levels compared to the *Fmr1* KO. The HET mice have downregulation of MMP-9 and full KO of FMRP. The PNN density is lower for the HET compared to the FMR KO based on Figure 4b and 4d. The results for PV density in the images for all genotypes suggests the PV cells are localized in the CA1 region.

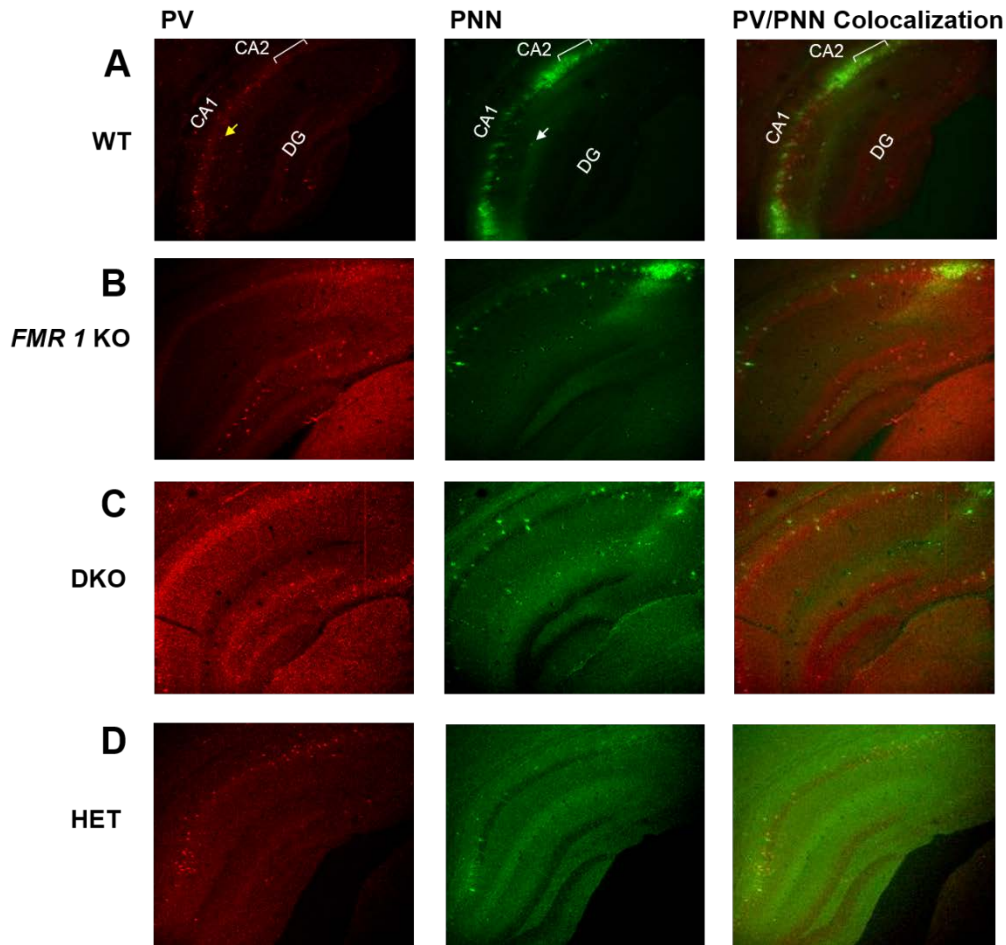


Figure 4. (A) (from left to right) Confocal laser-scanning microscopy images for WT and *FMR1* KO. The red channel represents PV cells (left), which are localized to the stratum pyramidale layer. The yellow arrow indicates one of the many PV cells. The green channel represents PNN labeling (middle). PNN indicated by the white arrow. The third image shows the colocalization between PV+ cells and PNN (right) (4 mice, 20 images, 20 z-stack overlay per image). The images have the CA1, CA2 and dentate gyrus (DG) identified on the image. The same region follows for the rest of the genotypes. (B) PV (left), PNN (middle), and PV/PNN colocalization in *Fmr1* KO mice (3 mice, 19 images, 20 z-stack overlay per image). (C) PV(left), PNN(middle), PV/PNN colocalization in DKO mice (4 mice, 19 images, 20 z-stack overlay per image). (D) PV(left), PNN(middle), PV/PNN colocalization in HET mice (4 mice, 16 images, 20 z-stack overlay per image).

PV/PNN Density Data

The confocal images were processed using Image J software and cells were counted using the cell counter analysis. Our first approach was to compare the PV cell and PNN density in the WT versus the *Fmr1* KO mice. The CA1 region showed a significant difference in PV cell density between the two genotypes (Figure 5d). The PV density in the *Fmr1* KO is less compared to the WT mice. There was also a significantly reduced number of PV cell containing PNN in *Fmr1* KO versus WT ($p < 0.001$). The CA1 exhibits less PNN density in the *Fmr1* KO compared to the wildtype but it is not a significant difference (Figure 5d). There is a difference between PNN and PV density in the CA2 region of the *Fmr1* KO mice but it is not statistically different from the WT mice (Figure 5c). In the CA3 and dentate gyrus there is no significant difference based on two-tailed t-test. The only significant difference is observed in the PV cell density in the DG and CA1 of *Fmr1* KO versus WT mice. Next, the DKO and HET mice were measured for PV and PNN density to determine if the removal of MMP-9 would rescue the phenotype observed in the *Fmr1* KO mice. We hypothesized that by removal of MMP9, which cleaves PNNs, would rescue the reduction of PNNs in *Fmr1* KO. As previously mentioned, there was not a significant difference in PNN levels in *Fmr1* KO mice compared to WT mice for all the regions of the hippocampus. Therefore, when measuring the PNN density for the DKO and HET mice, a form of rescue was not observed for all four genotypes. Based on one-way anova, the difference in PV and PNN density between all four genotypes, within the four subfields of the hippocampus, is not significant. There is also variability in the standard deviation between each genotype.

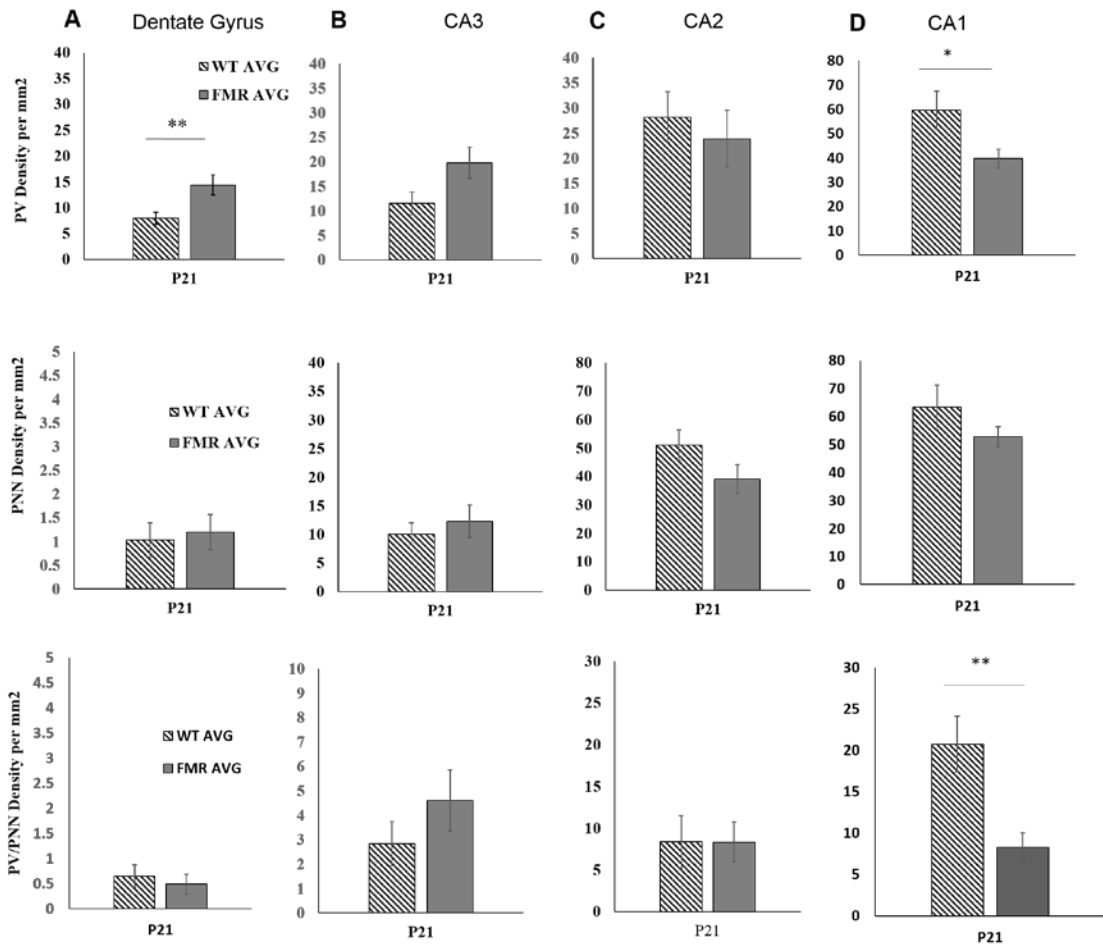


Figure 5. (A) The dentate gyrus showed a significant difference in PV cell density in WT vs *FMRI* KO (n = 20 for WT, n = 19 *FMRI* KO, P-value = 0.0065). PNN and PV/PNN colocalization showed no statically significant difference. (B) CA3 region of the hippocampus did not have significant statistical difference between WT and *FMRI* KO in PV/PNN cell density. (C) CA2 region showed no statistical significance in the difference of PV and PNN density in WT versus *FMRI* KO mice. (D) The CA1 region showed a difference in PV cell density between WT and *FMRI* KO (n = 20 WT, n=19 *FMRI* KO, P-value = 0.0336). There is also a significant difference in PV/PNN colocalization in WT versus *FMRI* KO (P-value = 0.0036).

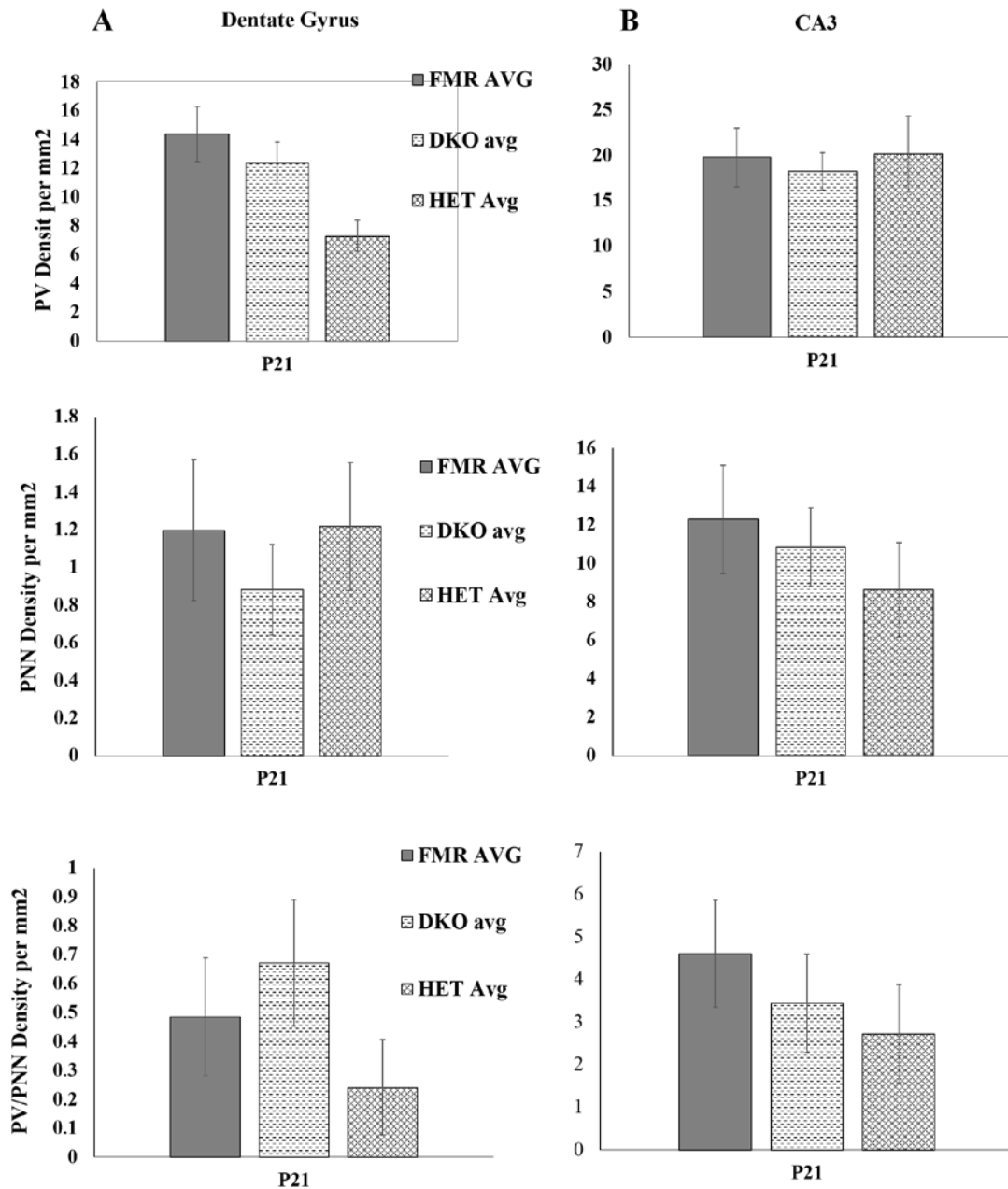


Figure 6. (A) The PV density (top left) in the DG region for the three genotypes. There was no significant difference or trend observed between the four groups. The PNN density (middle left) was also not significantly different for each of the genotypes. The standard deviation was significantly different. The PV/PNN colocalization (bottom left) was variable between the four genotypes, least in the HET mice (*Fmr1* KO n=19, DKO n=19, HET n=16). (B) The PV density (top right) in the CA3 region. There was no significant difference between the four genotypes. The PNN density (middle right) was about the same for the three groups. The PV/PNN colocalization (bottom right) showed no significant difference or trend based on the p-value. (significant p-value <0.05) No trend or significance was observed for the three groups of all regions of the hippocampus.

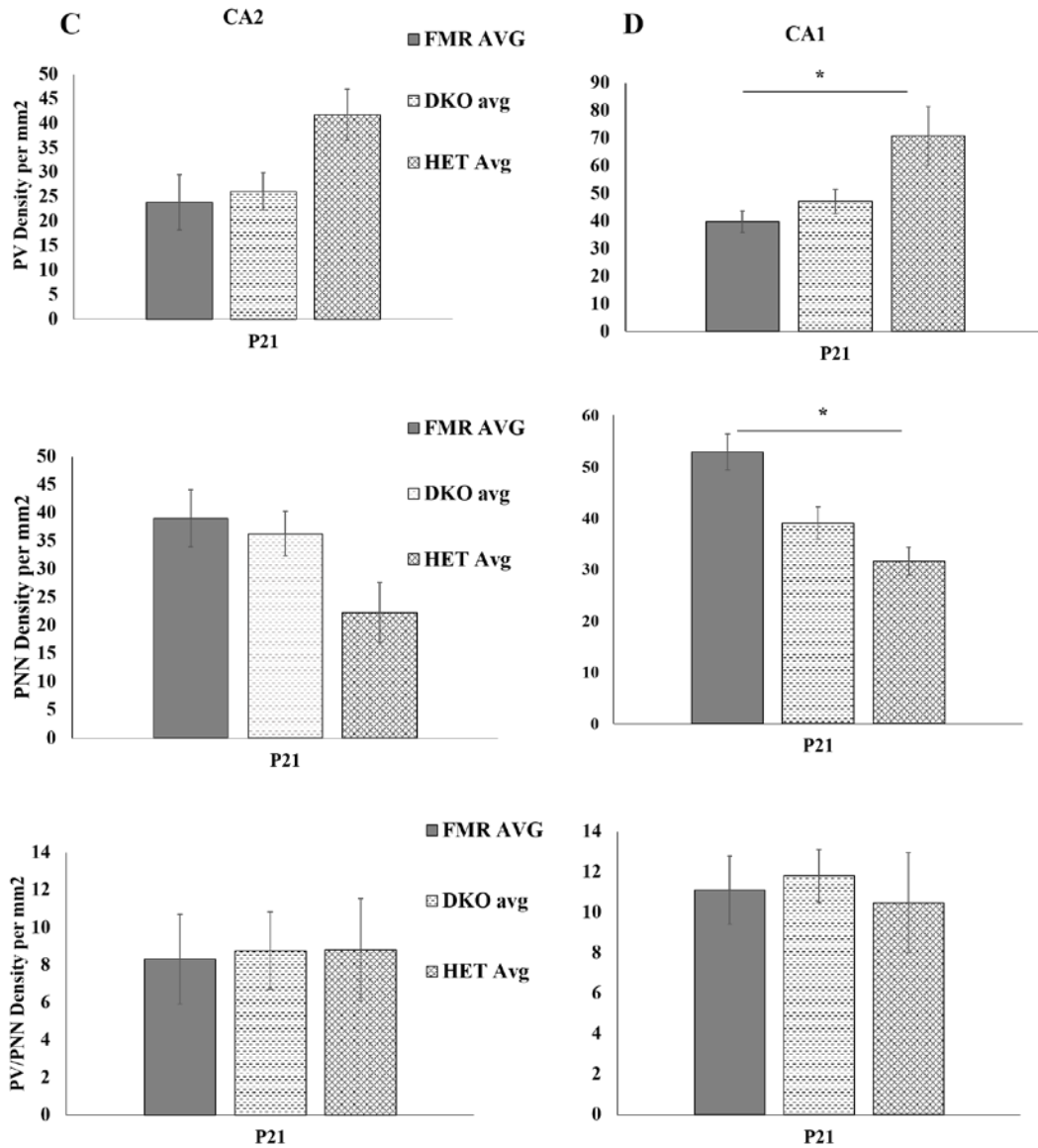


Figure 6. (C) The PV density (top left) in the CA2 region for the three genotypes. There was no significant difference or trend observed between the three groups. The PNN density (middle left) was also not significantly different for each of the genotypes. The standard deviation was significantly different. The PV/PNN colocalization (bottom left) showed similar levels for the three genotypes (*Fmr1* KO n=19, DKO n=19, HET n=16). (D) The PV density (top right) in the CA1 region. There was no significant difference between the four genotypes. The PNN density (middle right) was less in DKO and HET compared to *Fmr1* KO. This difference is not significant. The PV/PNN colocalization (bottom right) is similar in the *Fmr1* KO, DKO and HET mice. There is no significant difference or trend based on the p-value. (significant p-value <0.05).

DISCUSSION

Our study focused on the changes in PNN levels in different subfields of the hippocampus in a model of autism, specifically Fragile X Syndrome. FXS has many deficits including hypersensitivity, hyperexcitability and learning deficits (Wand et al., 2010). Some of these deficits have been thought to be associated with the E/I balance in synaptic circuits (Gogolla et al., 2009). *Fmr1* KO mice exhibit deficits in trace of fear memories (Hylín et al., 2013; Zhao et al., 2005). These deficits can result from the disruption of the PNNs in the CA1 subfield of the hippocampus (Hylín et al., 2013). As previously mentioned, the PNNs can function in the timing of the critical period and if disrupted can modify synaptic transmission (Pizzorusso et al., 2002). There is also evidence that suggests cell bodies of PV positive cells are mostly located in the stratum pyramidale layer of the hippocampus (Pawelzik et al., 2002). The PV positive cells are surrounded by PNNs which are thought to modify synaptic input directed to the inhibitory cells (Gogolla et al., 2009; Hylín et al., 2013).

Our experiments focused on P21 mice and the data suggests that the PV positive cells in CA1 subfield of the hippocampus are affected in *Fmr1* KO. By 21 days after birth, the mice have neared the end of the critical period and the change in inhibition can cause a learning deficits observed in *Fmr1* KO mice. This matches previous studies that indicate the PV cells are localized in the CA1 region of the stratum pyramidale layer in the hippocampus (Pawelzik et al., 2002). The CA1 region integrates multisensory excitatory input from the entorhinal cortex and indirect input from the CA3 (Basu et al., 2016). This area also has major GABAergic inputs, which provide local inhibition and this inhibition is key in the stability of synaptic transmission and consolidation of memory (Basu et

al.,2016; Hensch, 2005). As previously discussed, autism spectrum disorders such as FXS present a disruption in E/I circuit balance during development (Gogolla et al., 2009). Our data suggests there are less PV cells in the CA1 region in the *Fmr1* KO mice and this can affect the E/I circuit. This finding can be related to the idea that the E/I balance is affected in different forms of intellectual disability. We also see a specific loss of PNNs around PV positive cells in CA1 hippocampus of *Fmr1* KO mice. The CA1 subfield is divided into proximal and distal regions. Our results show significant differences in both regions. While CA1 distal is thought to be involved in object recognition task (Nakamura et al., 2013), CA1 proximal is associated with spatial memory along with connecting circuit from the CA3 subfield (Nakamura et al., 2013). There were no significant changes in PV or PNN levels observed in the CA3 area of the hippocampus for the different genotypes. We hypothesized that increased levels of MMP-9 in *Fmr1* KO mice can contribute to the reduced density of PNN-containing PV cells and reduced PV cell density in CA1 hippocampus. In previous studies, the MMP-9 levels were upregulated in the *Fmr1* KO mice but genetically reducing the MMP-9 levels rescued the FXS deficits (Sidhu et al., 2014). Studies comparing *Fmr1* KO versus DKO mice, showed that the DKO model experienced a rescued phenotype by exhibiting a reduced sensory processing deficit in the auditory cortex (Lovelace et al., 2016). Our data show an up-regulation of PV cell density, but not PNN-positive PV cell density, in CA1 hippocampus of MMP9^{+/-} *Fmr1* KO mice as compared to *Fmr1* KO mice, suggesting a possible role of MMP9 in regulating PV cell development/maturation in the CA1 hippocampus of *Fmr1* KO mice.

REFERENCES

1. Al-Hasani, R and Bruchas, MR 2011. Molecular mechanisms of opioid receptor-dependent signaling and behavior. *Anesthesiology* (2011).
2. Baker, K., Wray, S., Ritter, R., Mason, S., Lanthorn, T. and Savelieva, K.V. 2010. Male and female *Fmr1* knockout mice on C57 albino background exhibit spatial learning and memory impairments. *Genes, Brain and Behavior*. 9, 6 (2010), 562–574.
3. Basu, J, Zaremba, JD, Cheung, SK and Hitti, FL 2016. Gating of hippocampal activity, plasticity, and memory by entorhinal cortex long-range inhibition. *Science* (2016).
4. Brückner, G., Grosche, J., Hartlage-Rübsamen, M., Schmidt, S. and Schachner, M. 2003. Region and lamina-specific distribution of extracellular matrix proteoglycans, hyaluronan and tenascin-R in the mouse hippocampal formation. *Journal of Chemical Neuroanatomy*. 26, 1 (2003), 37–50.
5. Caruana, DA, Alexander, GM and Dudek, SM 2012. New insights into the regulation of synaptic plasticity from an unexpected place: hippocampal area CA2. *Learning & memory*. (2012).
6. Ding, Q., Sethna, F. and Wang, H. 2014. Behavioral analysis of male and female *Fmr1* knockout mice on C57BL/6 background. *Behavioural Brain Research*. 271, (2014), 72–78.
7. Dobkin, C., Rabe, A., Dumas, R., Idrissi, A., Haubenstock, H. and Brown, W. 2000. *Fmr1* knockout mouse has a distinctive strain-specific learning impairment. *Neuroscience*. 100, 2 (2000), 423–429.
8. Dölen, G, Carpenter, RL, O'Carroll, TD and Bear, MF 2010. Mechanism-based approaches to treating fragile X. *Pharmacology & therapeutics*. (2010).
9. Ethell, I. and Ethell, D. 2007. Matrix metalloproteinases in brain development and remodeling: Synaptic functions and targets. *Journal of Neuroscience Research*. 85, 13 (2007), 2813–2823.
10. Fagiolini, M, Fritschy, JM, Löw, K and Möhler, H 2004. Specific GABA_A circuits for visual cortical plasticity. *Science* (Mar. 2004).
11. Gogolla, N., LeBlanc, J., Quast, K., Südhof, T., Fagiolini, M. and Hensch, T. 2009. Common circuit defect of excitatory-inhibitory balance in mouse models of autism. *Journal of Neurodevelopmental Disorders*. 1, 2 (2009), 172–181.
12. Gogolla, N, Caroni, P, Lüthi, A and Herry, C 2009. Perineuronal nets protect fear memories from erasure. *Science*. (2009).
13. Harris, J., Hardie, N., Bermingham-McDonogh, O. and Rubel, E. 2005. Gene expression differences over a critical period of afferent-dependent neuron survival in the mouse auditory brainstem. *Journal of Comparative Neurology*. 493, 3 (2005), 460–474.
14. Hartig W, Derouiche A, Welt K, Brauer K, Grosche J, Mader M, et al. Cortical neurons immunoreactive for the potassium channel Kv3.1b subunit are predominantly surrounded by perineuronal nets presumed as a buffering system for cations. *Brain Res*.1999; 842:15–29.
15. Hensch, T.K. 2005. Critical period plasticity in local cortical circuits. *Nature reviews. Neuroscience*. 6, 11 (Nov. 2005), 877–88.
16. Hitti, F. and Siegelbaum, S. 2014. The hippocampal CA2 region is essential for social memory. *Nature*. 508, 7494 (2014), 88–92.

17. Hylin, M., Orsi, S., Moore, A. and Dash, P. 2013. Disruption of the perineuronal net in the hippocampus or medial prefrontal cortex impairs fear conditioning. *Learning & Memory*. 20, 5 (2013), 267–273.
18. Johnston, Daniel; Amaral, David G. Shepherd, Gordon M. (Ed). The synaptic organization of the brain, 5th ed. New York, NY, US: Oxford University Press (2014), pp. 455-498
19. Kazdoba, T., Leach, P., Silverman, J. and Crawley, J. Modeling fragile X syndrome in the *Fmr1* knockout mouse. *Intractable & Rare Diseases Research*. 3, 4 (2014), 118–133.
20. Lovelace, J.W., Wen, T.H., Reinhard, S., Hsu, M.S., Sidhu, H., Ethell, I.M., Binder, D.K. and Razak, K.A. 2016. Matrix metalloproteinase-9 deletion rescues auditory evoked potential habituation deficit in a mouse model of Fragile X Syndrome. *Neurobiology of disease*. 89, (May 2016), 126–35.
21. Murray, A., Woloszynowska-Fraser, M., Ansel-Bollepalli, L., Cole, K., Foggetti, A., Crouch, B., Riedel, G. and Wulff, P. 2015. Parvalbumin-positive interneurons of the prefrontal cortex support working memory and cognitive flexibility. *Scientific Reports*. 5, 1 (2015), 16778.
22. Nakamura, N., Flasbeck, V., Maingret, N., Kitsukawa, T. and Sauvage, M. 2013. Proximodistal Segregation of Nonspatial Information in CA3: Preferential Recruitment of a Proximal CA3-Distal CA1 Network in Nonspatial Recognition Memory. *The Journal of Neuroscience*. 33, 28 (2013), 11506–11514.
23. Neves, G, Cooke, SF and Bliss, T. 2008. Synaptic plasticity, memory and the hippocampus: a neural network approach to causality. *Nature Reviews Neuroscience*. (2008).
24. Pawelzik, H., Hughes, D. and Thomson, A. 2002. Physiological and morphological diversity of immunocytochemically defined parvalbumin- and cholecystokinin-positive interneurons in CA1 of the adult rat hippocampus. *Journal of Comparative Neurology*. 443, 4 (2002), 346–367
25. Pizzorusso, T., Medini, P., Berardi, N., Chierzi, S., Fawcett, J.W. and Maffei, L. 2002. Reactivation of ocular dominance plasticity in the adult visual cortex. *Science*. 298, 5596 (2002), 1248–1251.
26. Qin, M., Kang, J., Burlin, T., Jiang, C. and Smith, C. 2005. Post adolescent Changes in Regional Cerebral Protein Synthesis: An In Vivo Study in the *Fmr1* Null Mouse. *The Journal of Neuroscience*. 25, 20 (2005), 5087–5095.
27. Reinhard, SM and Razak, K 2015. A delicate balance: role of MMP-9 in brain development and pathophysiology of neurodevelopmental disorders. *Frontiers in cellular neuroscience*. (2015).
28. Rubenstein, J. and Merzenich, MM 2003. Model of autism: increased ratio of excitation/inhibition in key neural systems. *Genes*. (2003).
29. Sidhu, H., Dansie, L., Hickmott, P., Ethell, D. and Ethell, I. 2014. Genetic Removal of Matrix Metalloproteinase 9 Rescues the Symptoms of Fragile X Syndrome in a Mouse Model. *The Journal of Neuroscience*. 34, 30 (2014), 9867–9879.
30. Smit, A., Geest, J., Vellema, M., Koekkoek, S., Willemsen, R., Govaerts, L., Oostra, B., Zeeuw, C. and VanderWerf, F. 2008. Savings and extinction of conditioned eyeblink responses in fragile X syndrome. *Genes, Brain and Behavior*. 7, 7 (2008), 770–777.

31. Spencer, C., Alekseyenko, O., Hamilton, S., Thomas, A., Serysheva, E., Yuva-Paylor, L. and Paylor, R. 2011. Modifying behavioral phenotypes in *Fmr1*KO mice: genetic background differences reveal autistic-like responses. *Autism Research*. 4, 1 (2011), 40–56.
32. Till, S., Asiminas, A., Jackson, A., Katsanevaki, D., Barnes, S., Osterweil, E., Bear, M., Chattarji, S., Wood, E., Wyllie, D. and Kind, P. 2015. Conserved hippocampal cellular pathophysiology but distinct behavioural deficits in a new rat model of FXS. *Human Molecular Genetics*. 24, 21 (2015), 5977–5984.
33. Tsien, R. 2013. Very long-term memories may be stored in the pattern of holes in the perineuronal net. *Proceedings of the National Academy of Sciences*. 110, 30 (2013), 12456–12461.
34. Wang, LW, Berry-Kravis, E and Hagerman, RJ 2010. Fragile X: leading the way for targeted treatments in autism. *Neurotherapeutics*. (2010).
35. Zhao, M.-G., Toyoda, H., Ko, S., Ding, H.-K., Wu, L.-J. and Zhuo, M. 2005. Deficits in Trace Fear Memory and Long-Term Potentiation in a Mouse Model for Fragile X Syndrome. *The Journal of Neuroscience*. 25, 32 (2005), 7385–7392.